IV.C.5 Improving the Kinetics and Thermodynamics of $Mg(BH_4)_2$ for Hydrogen Storage

Brandon Wood (Primary Contact),
Lennie Klebanoff, Vitalie Stavila, Tae Wook Heo,
Keith Ray, Jonathan Lee, ShinYoung Kang,
Hui-Chia Yu, Katsuyo Thornton

Lawrence Livermore National Laboratory
7000 East Ave., L-413
Livermore, CA 94550
Phone: (925) 422-8391
Email: brandonwood@llnl.gov

DOE Manager: Jesse Adams
Phone: (720) 356-1421
Email: Jesse.Adams@ee.doe.gov

Subcontractors:
- Sandia National Laboratories, Livermore, CA
- University of Michigan, Ann Arbor, MI

Project Start Date: August 1, 2014
Project End Date: August 31, 2017

Overall Objectives

- Combine theory, synthesis, and characterization across multiple scales to understand the intrinsic kinetic and thermodynamic limitations in $MgB_2/Mg(BH_4)_2$.
- Construct and apply a flexible, validated, multiscale theoretical framework for modeling (de)hydrogenation kinetics of the Mg-B-H system and related metal hydrides.
- Devise strategies for improving kinetics and thermodynamics through nanostructuring and doping.

Fiscal Year (FY) 2016 Objectives

- Synthesize high-purity MgB_2 nanoparticles with size selectivity.
- Use theory-characterization feedback loop to understand chemical kinetic processes governing hydrogenation of MgB_2.
- Establish soft X-ray spectroscopic reference library to aid in identification of Mg-B-H intermediate phases.

Technical Barriers

This project addresses the following technical barriers from the Hydrogen Storage section of the Fuel Cell Technologies Office Multi-Year Research, Development, and Demonstration Plan.

(O) Lack of Understanding of Hydrogen Physisorption and Chemisorption

(A) System Weight and Volume

(E) Charging/Discharging Rates

Technical Targets

This project is conducting fundamental studies of hydrogenation and dehydrogenation of nanoscale $Mg(BH_4)_2$-based materials using a combined theory and experiment approach. Insights will be applied toward the design and synthesis of hydrogen storage materials that meet the following DOE hydrogen storage targets.

- Specific energy: 1.8 kWh/kg
- Energy density: 1.3 kWh/L
- Minimum delivery pressure: 5 bar
- Minimum delivery temperature: 85°C
- System fill time: 1.5 kg H_2/min

FY 2016 Accomplishments

- Demonstrated size-selective synthesis of MgB_2 nanoparticles with diameter <10 nm.
- Completed joint experiment-theory X-ray absorption spectroscopy (XAS) and X-ray emission spectroscopy (XES) studies of bulk material; computed library of spectra for intermediate identification with <1 eV agreement with measured references (completed go/no-go).
- Showed that high-pressure hydrogenation of MgB_2 can lead to direct conversion to $Mg(BH_4)_2$ with intermediates suppressed.
- Compared spectroscopic data with ab initio computations and kinetic analysis to show that hydrogenation of MgB_2 likely initiates at interfaces and defect sites.
- Completed bulk free energy and surface energy calculations for $Mg(BH_4)_2$ polymorphs, MgB_2, and commonly observed dehydrogenation intermediates for parameterization of kinetic models.

INTRODUCTION

$Mg(BH_4)_2$ is one of very few metal hydride candidates that lie close to the "viability window" of capacity (14.9 wt% H) and desorption enthalpy (ΔH_{des}) required to satisfy the 2020 and ultimate DOE hydrogen storage targets [1-2]. However, $Mg(BH_4)_2$ suffers from extremely poor kinetics whose origin is not well understood. If the kinetic limitations could be removed and the effective ΔH_{des} slightly improved, then facile hydrogen uptake and release could be attained, and a complex metal hydride-based system could achieve long-term targets. Prior work points to particle size reduction and doping with additives as viable and cost-effective improvement strategies [3]. However, it is difficult to fully leverage these without comprehending how, why, and under what conditions these improvements are observed. This project applies multiscale theoretical and experimental tools to develop a fundamental understanding of kinetic and thermodynamic limitations in the Mg-B-H hydrogen storage system, and to devise specific strategies for optimizing its performance under cycling conditions.

APPROACH

This project aims to establish a closely coupled theory/characterization/synthesis approach to understand the roles of nanostructuring and doping in the Mg-B-H system, and apply it to devise possible strategies for improving kinetics and thermodynamics. We focus on three objectives: (1) identifying chemical, phase nucleation, or transport processes and determining which are rate limiting; (2) understanding the origin of the kinetic and thermodynamic changes upon nanosizing and doping; and (3) devising and implementing rational modifications for improvement of H_2 storage properties. Our modeling effort relies on the application of a multiscale framework that combines atomistic density functional theory (DFT) for predictive chemistry and thermodynamics with continuum phase-field modeling for describing phase nucleation and growth and non-equilibrium transport kinetics. The predictions are informed and validated by controlled synthesis of size-selected nanoparticles free from binders and nanoscaffolds that may otherwise burden the system with unacceptably high gravimetric penalties. To better understand the kinetic pathways and processes, we apply gravimetric and thermochemical analysis, and utilize in situ and ex situ microscopy and spectroscopy aided by computational interpretations to derive chemical and phase compositions. Particular emphasis is placed on understanding kinetic factors governing the rehydrogenation of MgB_2, which is generally less well understood than dehydrogenation.

RESULTS

Improved thermodynamic predictions: A key goal of the project is the computation of more accurate thermodynamics of reactants, products, and intermediates in the Mg-B-H system, motivated by the need to reconcile discrepancies between experiments and theoretical predictions from DFT for the stability of reaction intermediates and pathways. We have been evaluating the possible relevance of three factors that are often neglected in DFT-computed reaction enthalpies: (1) explicit finite-temperature contributions to the free energy, including anharmonicity arising from B_xH_y molecular modes; (2) microstructural effects, including surface and interface contributions to the free energy; and (3) possible non-crystalline phases, including solid solutions, amorphous, and polycrystalline morphologies.

To address finite-temperature free energy contributions, we have applied a theoretical method being developed under HyMARC that separates contributions from the vibrational density of states within long ab initio molecular dynamics simulations [4]. This allows more accurate computation of entropic contributions rather than extrapolating from zero-temperature results. An added advantage is the ability to spatially decompose the entropy density to examine surface free energy contributions independently to predict size-dependent nanoparticle stability. Our calculations confirm that explicit calculations of the entropy can differ significantly from zero-temperature approximations (e.g., by 12 kJ/mol for β-$Mg(BH_4)_2$ at 600 K), with effects augmented at surfaces where molecular reorientations are minimally constrained.

Surface energies were also computed for several of the known phases (see examples in Table 1). These surface energies were then averaged according to the Wulff construction to better represent the variety of likely crystallite domain geometries, and were computed at the limits of low and high chemical potentials of Mg. These energies are currently being used as the basis for initial estimates of interfacial energies for inclusion within the HyMARC phase fraction prediction code. They are also being used to compute nucleation barriers and critical nucleus sizes for each of the phases, which gives a way to connect size-dependent thermodynamics directly to phase kinetics. For instance, high MgB_2 surface energy implies high interface energies and nucleation barriers, which may help to explain the difficulty in fully dehydrogenating $Mg(BH_4)_2$. These computations will be a key focus as validation data on MgB_2 nanoparticles becomes available.

Measured and computed X-ray spectroscopy for intermediate identification: XAS and X-ray emission spectroscopy (XES) can provide information about local electronic structure, which can be used alongside nuclear magnetic resonance and vibrational spectroscopy to identify intermediates and understand phase evolution. XAS and XES

TABLE 1. Calculated Surface Energies for Select Mg-B-H Compounds

Phase	Surface Orientation	σ (J/m^2)	Phase	Surface Orientation	σ (J/m^2)
γ-$Mg(BH_4)_2$	{111}	0.22	MgB_2	{1-100}	4.04
	{110}	0.22		{0001} Mg line	1.82
β-$Mg(BH_4)_2$	{010} term 1	0.57		{0001} Mg diamond	1.82
	{010} term 2	3.43		{0001} B line	5.18
$MgB_{12}H_{12}$	{100}	0.13		{0001} B diamond	7.77
	{010}	0.01		{0001} B zigzag	2.18
	{001} Mg line	0.15		{11-20}	2.40
	{001} Mg para	0.12		{1-101}	1.80
	{001} BH line	0.65	MgH_2	{100}	0.94
	{001} BH zigzag	0.26		{001}	0.84
				{101}	3.12

are particularly useful for probing MgB_2, since it features delocalized electronic states that differ qualitatively from insulating $Mg(BH_4)_2$ and the ionic salts proposed as reaction intermediates. Using methods described in Prendergast, et al. [5], we simulated XAS and XES spectra of $Mg(BH_4)_2$, MgB_2, and intermediates predicted near the convex hull in the calculations of Zhang et al. [6]. Averages over ab initio molecular dynamics simulations were used to account for thermal effects. In collaboration with HyMARC, these were compared with measured spectra on select single-phase samples to establish the validity of the combined experiment-theory spectroscopy approach and build a library of reference spectra for interpreting intermediates. Once proper protocols for controlling oxidation during sample handling were established, we found <1 eV agreement between the measured and computed reference spectra, fulfilling our go/no-go requirement (see Figure 1). The predictive capability of the computational approach ensures it can confidently be applied to phases and configurations that cannot be experimentally isolated in pure form. Discernible differences

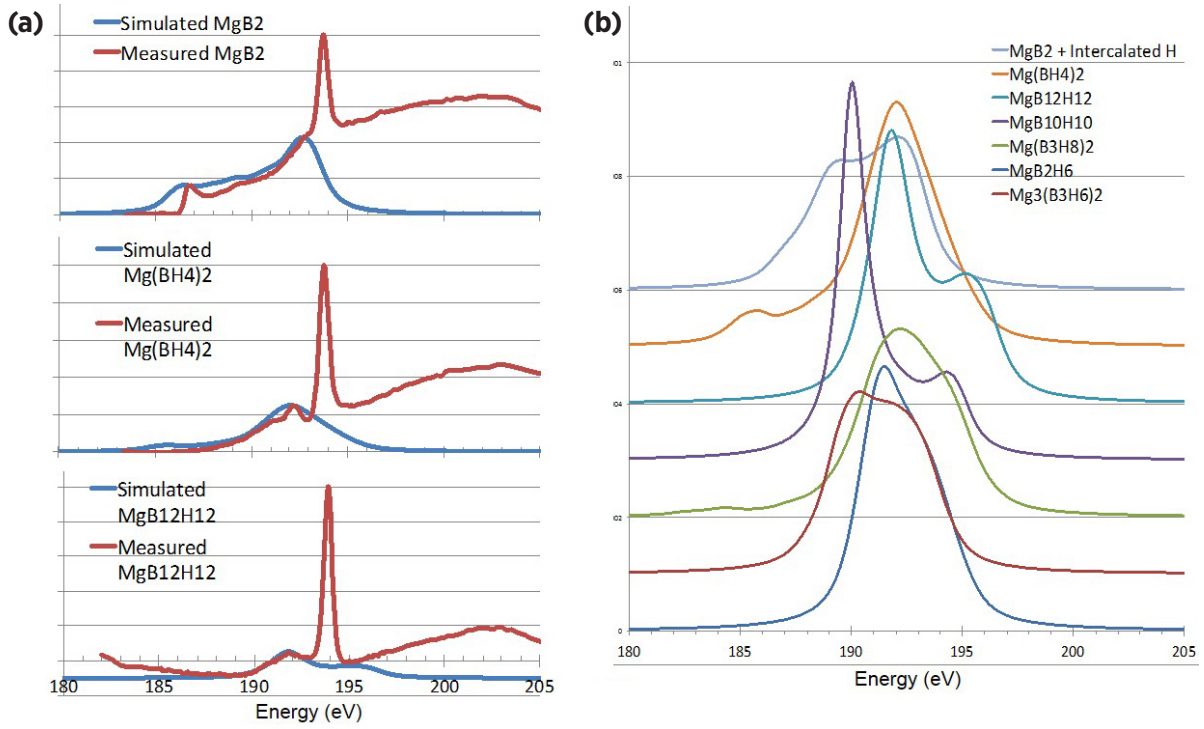

FIGURE 1. (a) Comparison between simulated (blue) and measured (red) XAS spectra at the boron K-edge, showing similar resonances to within ~1 eV (the sharp peak below 194 eV in the experimental spectrum is oxide-derived); (b) Calculated boron K-edge XAS spectra for intermediate phases at 300 K.

between the XAS and XES spectra also confirm the technique's usefulness for identifying intermediate species.

Understanding chemical kinetic processes in (de) hydrogenation: Our kinetics studies have been broadly aligned along two aspects: first, understanding chemical changes with hydrogen composition within single phases; and second, understanding structural phase transitions between different phases. The first is based on combining ab initio chemical modeling and spectroscopy, and the second combines phase-field kinetic modeling with experimental phase discrimination. Whereas the structural phase transitions were a key focus of the previous year, this year's primary focus has been on understanding chemical changes in single-phase regimes. Particular emphasis has been placed on elucidating kinetic processes and mechanisms during the initial hydrogenation of MgB_2, which remain poorly understood.

We applied a more detailed kinetic analysis to MgB_2 hydrogen uptake curves measured within a Sieverts apparatus at P = 145 bar H_2 (T = 364°C, 378°C, and 391°C; total uptake ~0.85 wt% H) by using Arrhenius fitting to extract separate barriers *for each level of hydrogenation* (Figure 2).

The quality of the Arrhenius fits were also recorded as a measure of the heterogeneity of the process, since non-Arrhenius behavior is typical of processes with a variety of barriers. The initial uptake region (< 0.25 wt% H) is non-Arrhenius, leading us to suspect that it represents the initial dissociation of H_2 at heterogeneous surface sites. The corresponding barrier is also quite similar to the dissociation barrier of 0.89 eV computed by Wang et al. [7]. From 0.2 wt% H to 0.7 wt% H, the behavior is more regular, and likely indicates a diffusive and/or reactive regime. This analysis confirms the presence of multiple governing processes in initial hydrogenation.

To understand these processes in more detail, we applied synchrotron soft X-ray spectroscopy, Fourier transform infrared spectroscopy, and nuclear magnetic resonance to the initially hydrogenated (0.85 wt% H) MgB_2 samples (Figure 3). Comparison with reference XAS spectra showed that there is a signature in the boron K-edge XAS spectrum that is unique to MgB_2, whose disappearance can be tracked to indicate transitions to other chemical environments (marked with * in Figure 3b). This spectral signature is only weakly affected by the introduction of hydrogen, which suggests very few boron atoms exist in an altered chemical environment. This implies concentration of hydrogen at a small number of sites where boron is highly hydrogenated. To illustrate this point, consider that conversion to lower hydrogenation states in the form of $MgB_{12}H_{12}$ or homogeneously dispersed B-H bonds should theoretically result in a ~20% reduction in intensity of the key spectral signature (*). In addition, comparison with our single-phase reference spectra showed no signatures specific to

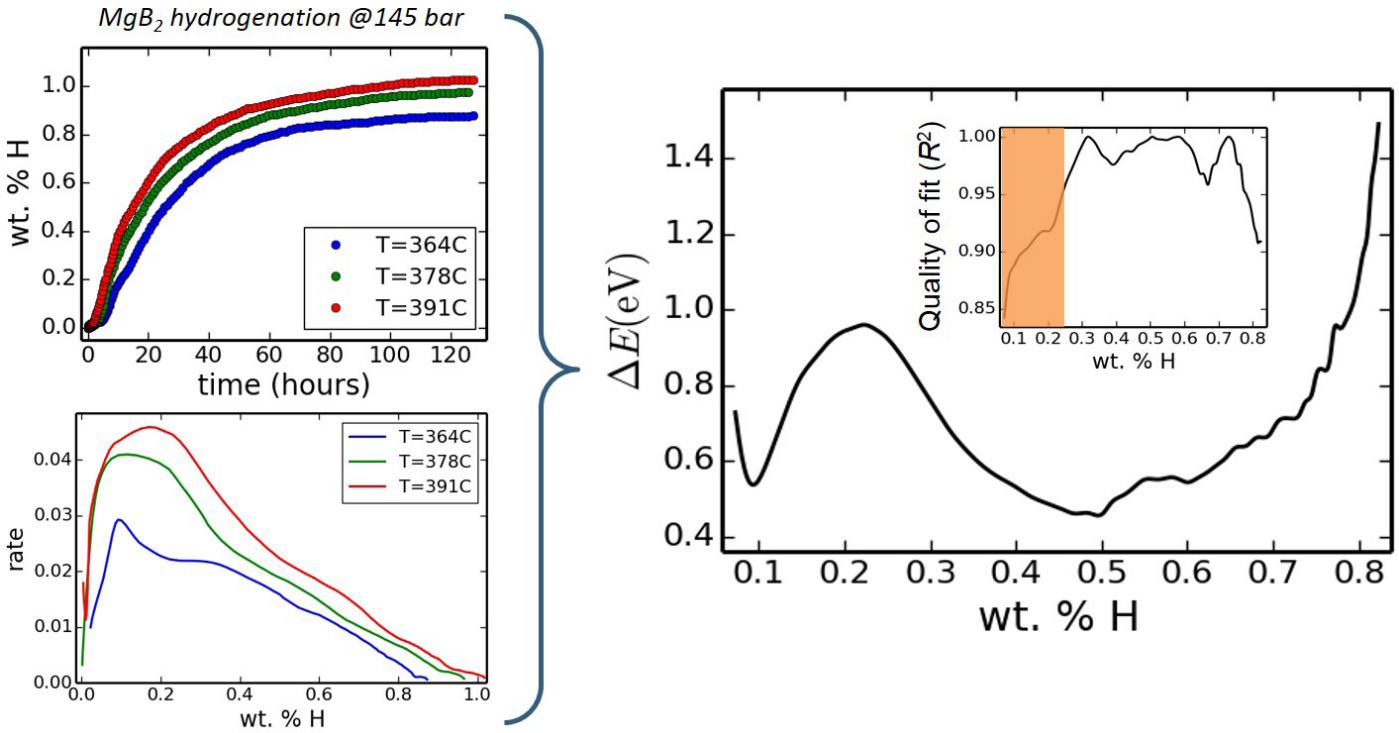

FIGURE 2. Arrhenius kinetic analysis of the isotherm uptake curves and corresponding rates for MgB_2 at 145 bar (left panels). The inset of the right-hand figure shows the quality of the Arrhenius fits, from which it is clear that early reaction stages (< 0.25 wt%H) are dominated by non-Arrhenius processes indicative of significant heterogeneity.

intermediates (e.g., $MgB_{12}H_{12}$). At the same time, the Fourier transform infrared spectrum for the initially hydrogenated sample (Figure 3c) shows features consistent with a linear mixture of MgB_2- and $Mg(BH_4)_2$-like spectra. Again, no features corresponding to $B_{12}H_{12}$ or dispersed B-H bonds are detected. We conclude that initial MgB_2 hydrogenation manifests as direct conversion to a BH_4-like coordination environment.

To better interpret the microscopic details of the MgB_2 hydrogenation process and understand the underlying spectral features, we performed a series of first-principles calculations of the energetics, electronic structure, and XAS and XES spectra of possible model interaction geometries. By directly comparing the computed and measured spectra, we were able to judge which of the models are compatible with our experimental samples. A comparison between the computed XAS spectrum for MgB_2 and the electronic density

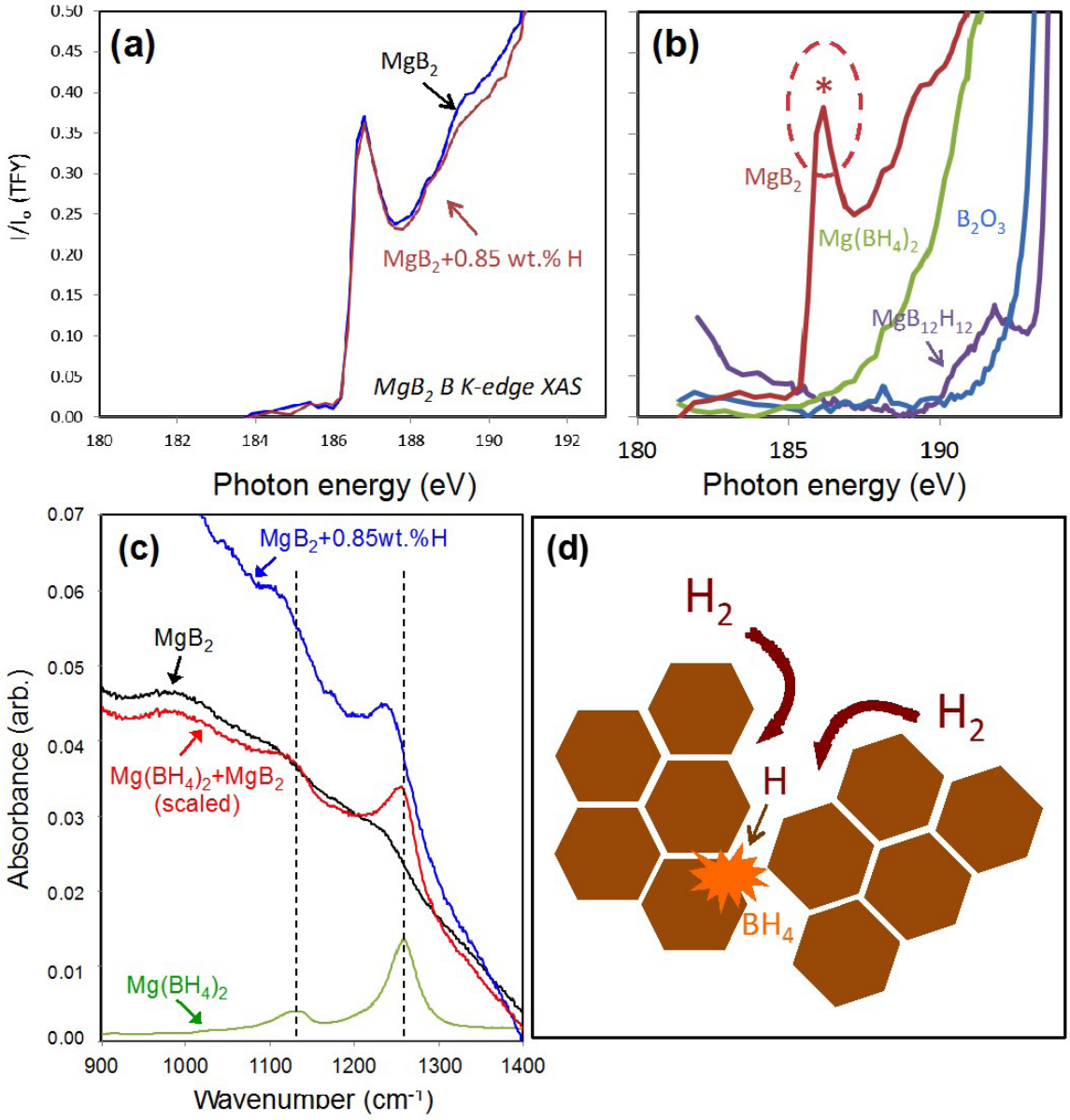

FIGURE 3. (a) XAS spectra at the boron K-edge for pure and partially hydrogenated MgB_2 (0.85 wt% H); (b) XAS spectrum for MgB_2 compared to reference spectra for B_2O_3, $MgB_{12}H_{12}$, and $Mg(BH_4)_2$, showing the signature boron p_{xy} spectral feature (*) unique to MgB_2; (c) Fourier transform infrared spectrum of partially hydrogenated MgB_2 (0.85 wt% H; blue), compared to reference $Mg(BH_4)_2$ (green), MgB_2 (black) spectra, and a linear $Mg(BH_4)_2/MgB_2$ mixture with the expected stoichiometric ratio (red); (d) Proposed mechanism of initial hydrogenation of MgB_2, in which hydrogen dissociates and diffuses rapidly along interfaces and grain boundaries to collect at high-energy bonds and directly form highly coordinated BH_4-like molecular complexes.

of states showed that the (*) feature in Figure 3b is actually a signature of the boron p_{xy} state, which disappears if this state is disrupted by hydrogen bonding. Using this understanding as a guide, we set about computationally testing specific sites for hydrogen incorporation and comparing their spectra to the measured ones. The most intuitive structure involved atomic hydrogen incorporation into the bulk material. The most stable bulk site involves intercalation of H between Mg and B planes; however, this was very energetically unfavorable with respect to H_2 (+1.3 eV/H), meaning there is no thermodynamic basis for H incorporation into the ideal structure. Computing the XAS spectrum further allowed us to confirm that H incorporation into bulk MgB_2 is incommensurate with the experimental data, since even small amounts of hydrogen significantly impact the boron p_{xy} feature as hydrogen donates electrons into the boron sheets.

Since bulk intercalation of atomic hydrogen does not fit the data, we instead computed energetics of hydrogen insertion at edges and surfaces, which we used as simple models for solid-state interfaces. We find that these sites are significantly more favorable (about -0.8 eV per H for edges and -0.5 eV per H for surfaces). We conclude that high-energy B-B bonds at interfaces are the likely targets for initial hydrogenation, and that these bonds act as magnets for subsequent hydrogen atoms to form highly coordinated BH_4 complexes. Morevoer, these sites already have highly strained and irregular electronic orbitals, which explains why hydrogenation initially has little impact on the boron p_{xy} states in this case. These interfaces and grain boundaries were also predicted in our calculations to be the preferred diffusion pathways for atomic hydrogen, which rationalizes our uptake results with prior computational studies suggesting bulk diffusion should be nearly impossible under these conditions [8]. The combined experiment and theory investigation therefore points to the scenario shown in Figure 3d, with hydrogenation initiating at grain boundaries or interfaces and "etching" the boron from these edges inward [9]. Notably, this mechanism is fundamentally different from the dehydrogenation process, and suggests that $Mg(BH_4)_2$ can be directly upon hydrogenation of MgB_2 without significant intermediates. It also suggests higher relative surface and interface volume (e.g., in nanoparticles) should improve MgB_2 uptake kinetics. Our spectral interpretation remainined consistent for samples hydrogenated up to 7 wt% H at higher pressure (700 bar).

We have also been running ab initio quantum molecular dynamics to obtain direct insights into the chemistry and transport processes active during the initial dehydrogenation of β-$Mg(BH_4)_2$. These computations are intensive, but can be extremely informative and account directly for finite-temperature kinetic effects inaccessible to more conventional calculations. The example in Figure 4 shows B-H bond activation at a (001) surface of β-$Mg(BH_4)_2$. This process is difficult in the bulk material owing to the rigidity of the Mg^{2+} coordination environment, but becomes feasible at surfaces and interfaces due to spontaneous surface disordering. Because BH_4 rotational disorder and B-H bond activation are necessary ingredients for structural diffusion, their manifestation in the finite-temperature simulation implies a facile surface–interfacial hydrogen transport pathway. This contrasts with the >2 eV barrier predicted by Wolverton and Ozoliņš for vacancy-driven transport in an ideal bulk crystal of $Mg(BH_4)_2$ [8], and is instead more consistent with isotope exchange measurements [10].

Modeling multiphase kinetics: Our phase kinetics modeling efforts have proceeded along three fronts:

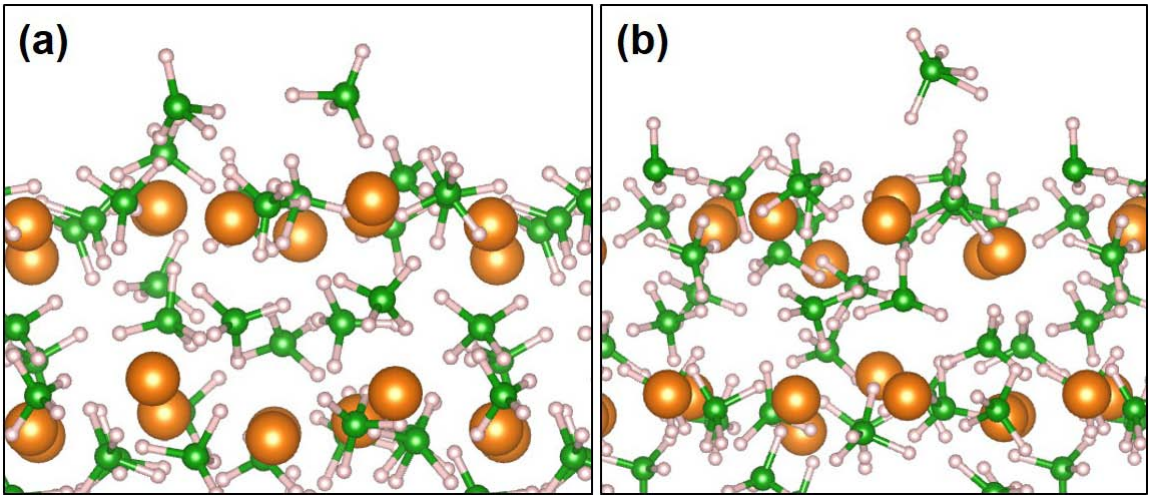

FIGURE 4. Signature of structural diffusion of hydrogen at a surface of β-$Mg(BH_4)_2$ taken from ab initio molecular dynamics of a (001) surface at 800 K. Surface disordering facilitates interaction between the two BH_4^- polyhedra in the left panel, leading to B-H bond activation and hydride transfer. In this instance, the process is accompanied by Mg^{2+} reduction (not shown).

nucleation modeling, stability analysis based on microstructure, and phase-field modeling of full reaction kinetics. First, we have used the DFT-computed surface energies s_i to estimate interfacial energies g_{ij} using a semi-empirical approximation derived from grain boundary models [11], in which $g_{ij} = p\,(s_i + s_j)$. Instead of fitting the constant *p*, our approach tests a range of values (e.g., from 0.3 to 0.7) to extract reasonable ranges of possible interfacial energies. These interfacial energies were used within classical nucleation theory to estimate ranges of homogeneous and heterogeneous nucleation barriers for the various phases in Mg- or B-rich conditions. The smallest stress-free homogenous nucleation barrier was found for $MgB_{12}H_{12}$ (below 1 meV) and the largest for MgB_2 (up to 600 meV), which may explain the difficulty in forming the latter phase upon dehydrogenation. However, stress factors, which are neglected in the current model, are likely to significantly penalize nucleation of the lower-density intermediate phases such as $MgB_{12}H_{12}$ due to the accompanying volume expansion, which along with diffusion limitations may favor observation in amorphous or solid solution forms.

Second, in collaboration with HyMARC, we have developed an extension to the Grand Canonical Linear Programming method [12] that takes into account the microstructure and interfacial energies associated with multiphase coexistence. These corrections are expected to play an increasingly important role in nanoparticle systems, which will be studied in detail in the next project phase. We have applied this formalism to model reactions and microstructures in the Mg-B-H as proof of concept, but will return to this effort as our characterization reveals further evidence of the relevant phases and microstructures that need to be considered during operating conditions.

Third, again in collaboration with HyMARC, we have been developing a phase-field model for reaction kinetics based on previously demonstrated methods. The Mg-MgH_2 portion of the phase diagram is being modeled with an interstitial hydride model [13], whereas all other relevant reactions are considered by adapting a multiphase conversion model previously developed for battery materials [14]. Although early feasibility tests are promising, this model requires parameterization of the free energy surface for the single-phase and multi-phase regions of the phase diagram, which rely on further parameterization from the additional experiments and computations being performed as part of the project. Demonstration of this integrated model will meet our final project milestone.

Size-selective MgB_2 nanoparticle synthesis: Our progress in understanding the bulk material has set the stage for the next phase of the project focusing on nanoscale materials. To this end, we have also been working to synthesize phase-pure MgB_2 nanoparticles with narrow size distributions. Specifically, we developed a new approach for the synthesis of MgB_2 nanoparticles using surfactant-assisted ball-milling. The method consists of milling MgB_2 powder in the presence of oleic acid and oleylamine in a hydrocarbon such as hexane or heptane. The powders were milled using a SPEX-8000 high-energy mill. We optimized the milling conditions to allow the synthesis of sub-50 nm nanoparticles, which can be easily separated from the reaction mixture. Scanning transmission electron microscopy imaging confirmed agglomerates of small particles, with the size histogram indicating most of the particles are 10–20 nm in diameter. The particles can be purified by washing and centrifugation steps in the presence of ethanol. We plan to explore surfactant removal techniques to control the surface chemistry of the MgB_2 nanoparticles for subsequent hydrogenation tests.

CONCLUSIONS AND FUTURE DIRECTIONS

- High-pressure hydrogenation of MgB_2 can lead to direct conversion to $Mg(BH_4)_2$ with intermediates suppressed, suggesting different phase pathways for hydrogenation and dehydrogenation.
- Feedback loop between theory and experimental characterization was used to show that MgB_2 hydrogenation likely initiates at interfaces and defect sites, suggesting morphological and microstructural engineering could improve kinetics.
- *Future direction*: Refine nanoparticle synthetic procedures for higher phase purity and repeat spectroscopic characterization of nanoparticles for comparison to predictions.
- *Future direction:* Complete quantitative assessment of the importance of "beyond-ideal" contributions to the computed thermodynamics of reactants, products, and intermediates, including anharmonicity, morphology, and microstructural considerations in bulk and nanoscale materials.
- *Future direction:* Perform high-temperature ab initio molecular dynamics of phase mixtures to identify additional possible chemical pathways.
- *Future direction:* Complete and validate reactive-diffuse interface model for inclusion in phase-field framework.

FY 2016 PUBLICATIONS/PRESENTATIONS

1. Wood, B.C. et al. "Improving the kinetics and thermodynamics of $Mg(BH_4)_2$ for hydrogen storage." *U.S. DOE Hydrogen and Fuel Cells Program Annual Merit Review*, Washington, D.C., June 2016.

2. Stavila, V. et al., "Understanding and controlling hydrogen release and uptake in complex metal hydrides," *Pacifichem*, Honolulu, HI, December 2015.

3. Wood, B.C. et al., "Nanointerface-driven reversible hydrogen storage in the nanoconfined Li-N-H system," *Materials Research Society Spring Meeting*, Phoenix, AZ, April 2016.

4. Wood, B.C., V. Stavila, N. Poonyayant, T.-W. Heo, K. Ray, L.E. Klebanoff, T.J. Udovic, J. Lee, N. Angboonpong, J.D. Sugar, and P. Pakawatpanurut. "Nanointerface-driven reversible hydrogen storage in the nanoconfined Li-N-H system." *Submitted* (2016).

REFERENCES

1. Klebanoff, L.E., and J.O. Keller. "5 Years of hydrogen storage research in the US DOE Metal Hydride Center of Excellence (MHCoE)." *Int. J. Hydr. Energy* 38 (2013): 4533–4576.

2. Pasini, J.M., C. Corgnale, B.A. van Hassel, T. Motyka, S. Kumar, and K.L. Simmons. "Metal hydride material requirements for automotive hydrogen storage systems." *Int. J. Hydr. Energy* 38 (2013): 9755–9765.

3. Fichtner, M., Z. Zhao-Karger, J. Hu, A. Roth, and P. Weidler. "The kinetic properties of $Mg(BH_4)_2$ infiltrated in activated carbon." *Nanotechnology* 20 (2009): 204029.

4. Teweldeberhan, A.M. and S.A. Bonev. "Structural and thermodynamic properties of liquid Na-Li and Ca-Li alloys at high pressure." *Phys. Rev. B* 83 (2011): 134120.

5. Prendergast, D., and G. Galli. "X-ray absorption spectra of water from first principles calculations." *Phys. Rev. Lett.* 96 (2006): 215502.

6. Zhang, Y., E. Majzoub, V. Ozoliņš, and C. Wolverton. "Theoretical Prediction of Metastable Intermediates in the Decomposition of $Mg(BH_4)_2$." *J. Phys. Chem. C* 116 (2012): 10522–10528.

7. Wang, Y., K. Michel, Y. Zhang, and C. Wolverton. "Thermodynamic stability of transition metals on the Mg-terminated MgB2 (0001) surface and their effects on hydrogen dissociation and diffusion." *Phys. Rev. B* 91 (2015): 155431.

8. Wolverton, C., et al. *U.S. DOE Hydrogen and Fuel Cells Program Annual Report* (2013).

9. Ray, K.G., J.R.I. Lee, L.E. Klebanoff, V.N. Stavila, T.W. Heo, S. Kang, and B.C. Wood. "Key mechanisms in the initial hydrogenation of MgB_2." *Manuscript in preparation* (2016).

10. Hagemann, H., V. D'Anna, J.-P. Rapin, and K. Yvon. "Deuterium-hydrogen exchange in solid $Mg(BH_4)_2$." *J. Phys. Chem. C* 114 (2010): 10045–10047.

11. Porter, D.A., and K.E. Easterling, *Phase Transformations in Metals and Alloys.* 2nd ed.; Chapman & Hall: London, UK (1992).

12. Akbarzadeh, A.R., V. Ozoliņš, and C. Wolverton. "First-Principles Determination of Multicomponent Hydride Phase Diagrams: Application to the Li-Mg-N-H System." *Adv. Mater.* 19 (2007): 3233–3239.

13. Voskuilen, T.G., and T.L. Pourpoint. "Phase field modeling of hydrogen transport and reaction in metal hydrides." *Int. J. Hydrogen Energy* 38 (2013): 7363–7375.

14. Yu, H.-C., F. Wang, G.G. Amatucci, and K. Thornton. "A phase-field model and simulation of kinetically asymmetric ternary conversion-reconversion transformation in battery electrodes." *J. Phase Equil. Diff.* 37 (2016): 86–89.